

International Journal of Modern Physics A  
 © World Scientific Publishing Company

## Associated production of $J/\psi$ and direct photon in the NRQCD and the ICEM using the high-energy factorization

Lev Alimov

*Samara National Research University, Moskovskoe Shosse, 34, 443086, Samara, Russia.  
 alimov.le@yandex.ru*

Anton Karpishkov

*Samara National Research University, Moskovskoe Shosse, 34, 443086, Samara, Russia*

*Joint Institute for Nuclear Research, Dubna, 141980 Russia.  
 karpishkoff@gmail.com*

Vladimir Saleev

*Samara National Research University, Moskovskoe Shosse, 34, 443086, Samara, Russia*

*Joint Institute for Nuclear Research, Dubna, 141980 Russia.  
 saleev.vladimir@gmail.com*

We study the associated  $J/\psi$  and direct photon production in the high-energy factorization, as it is formulated in the parton Reggeization approach, using two different models for the hadronization of a heavy quark-antiquark pair into a heavy quarkonium, namely the non-relativistic quantum chromodynamics (NRQCD) and the improved color evaporation model (ICEM). We find essential differences in the predictions for cross-section and transverse momenta spectra obtained using the NRQCD and the ICEM, which can be used to discriminate between these models. Our prediction for cross-sections of the associated  $J/\psi$  and direct photon production at the LHC energies slightly overestimates the results obtained early in the next-to-leading order (NLO) calculation in the collinear parton model (CPM). We predict different two-particle correlation spectra in the associated  $J/\psi$  and direct photon production which may be of interest for experimental study.

### 1. Introduction

The experimental study of the associated production of  $J/\psi$ -meson and direct photon production in high energy proton-proton collisions is of considerable interest, not only for verifying the predictions of the perturbative quantum chromodynamics (QCD) and various models of heavy quark hadronization into heavy quarkonium,<sup>1,2</sup> but also for obtaining information about the gluon parton distribution function (PDF) of a proton, including the transverse momentum dependent (TMD) gluon PDFs.<sup>3,4</sup>

The value of the strong coupling constant at the scale of a charm quark mass

$\alpha_S(m_c) \simeq 0.3$  is small enough to use perturbative QCD calculations to describe the charmonium production. At present, an accuracy level corresponding to next-to-leading order (NLO) in  $\alpha_S$  calculation based on the collinear parton model (CPM) has been achieved for the prompt  $J/\psi$  production<sup>5</sup> as well as for associated  $J/\psi$  and direct photon production.<sup>6</sup>

The process of hadronization of a  $c\bar{c}$ -pair into the charmonium state has a non-perturbative nature that can be described only within the framework of phenomenological models. In the color singlet model (CSM),<sup>7,8</sup> it is assumed that a quark-antiquark pair forms a color singlet state with quantum numbers of the final charmonium. In a more general framework of the non-relativistic quantum chromodynamics (NRQCD), which takes into account relativistic corrections in terms of the relative velocities of the quark and anti-quark inside the charmonium, the production of charmonium may be via color-octet intermediate states.<sup>9</sup> Another approach to describe the hadronization is the color evaporation model (CEM). It assumes that all quark-antiquark pairs with an invariant mass between the thresholds for the charmonium production and the open charm production convert into bound charmonium states  $\mathcal{C}$ , with a certain  $F^{\mathcal{C}}$  conversion probability.<sup>10,11</sup> Nowadays, the improved CEM (ICEM) has been suggested by Ma and Vogt in Ref.<sup>12</sup>

The crown stone in describing the charmonium production in high energy proton-proton collisions is the factorization of a hard and a soft physics phenomena. At the high transverse momentum, ( $p_T \gg m_C$ ), where the initial parton transverse momenta may be neglected, the charmonium production in the proton-proton hard collisions can be described adequately within the CPM.<sup>13</sup> However, to describe  $p_T$ -spectrum at low the transverse momentum ( $p_T \ll m_C$ ), the approach must be depended on a non-perturbative transverse momenta of the initial partons. This is achieved by using the transverse momentum dependent (TMD) factorization approach, well-known as the TMD parton model, which takes the effects of intrinsic parton motion into account.<sup>14</sup> To describe the experimental data in the intermediate range of transverse momenta,  $p_T \simeq m_C$ , different methods are used, combining the results of calculations based on the CPM and TMD PM.<sup>15</sup> At high energies, an alternative method for describing the cross-section across in the entire range of  $p_T$  is using the parton Reggeization approach (PRA).<sup>16-18</sup> The PRA is a version of the high-energy factorization (HEF) formalism, which is based on the modified multi-Regge kinematics (MRK) approximation of the QCD when we deal with the Reggeization of parton amplitudes. In the PRA, we have described early the experimental data for prompt and direct  $J/\psi$  production at the energies  $\sqrt{s} = 1.8 - 13$  TeV using the NRQCD approach<sup>19-21</sup> as well as using the ICEM.<sup>22</sup>

At present, a significant amount of experimental data has been collected for the production of prompt  $J/\psi$ -mesons in hadronic interactions at energies ranging from  $\sqrt{s} = 19$  GeV to  $\sqrt{s} = 13$  TeV.<sup>23</sup> The production of a single direct photons in hadron-hadron collisions has been extensively studied experimentally over a wide range of energies at the fixed target experiments<sup>24</sup> and at the RICH, Tevatron and

LHC colliders.<sup>25–27</sup> In the PRA, we studied single, double, and triple isolated photon production at the LHC in Refs.<sup>28–31</sup>

However, to date, no measurements have been made for the associated  $J/\psi$  and direct photon production cross-sections. In this paper, we study the associated production of  $J/\psi$ -meson and direct photon using the HEF, as it is formulated in the PRA, using two different models for the heavy quark hadronization into heavy quarkonium states, namely the NRQCD and the ICEM. We predict the cross-section and relevant spectra of  $J/\psi$  and direct photon pairs in proton-proton collisions at the energy  $\sqrt{s} = 13$  TeV.

## 2. Parton Reggeization Approach

The PRA is a gauge-invariant version of the  $k_T$ -factorization approach, which has been proven in the leading logarithmic approximation (LLA) of the high energy QCD.<sup>32–34</sup> The crown stones of the PRA are amplitude factorization in the Regge limit of the QCD (amplitude Reggeization), the Effective Field Theory (EFT) of Reggeized gluons and Reggeized quarks, proposed by Lev Lipatov in Ref.,<sup>35</sup> and the modified Kimber-Martin-Ryskin-Watt (KMRW)<sup>36,37</sup> model for unintegrated parton distribution functions (uPDF).<sup>18</sup>

In the PRA, the cross-section of the process direct  $J/\psi$  production together with large- $p_T$  photon,  $pp \rightarrow J/\psi\gamma X$ , is expressed as a convolution of the relevant Reggeized parton-parton cross-section and uPDFs. For example, for the gluon-gluon fusion subprocess we can write:

$$d\sigma(pp \rightarrow J/\psi\gamma X) = \int \frac{dx_1}{x_1} \int \frac{d^2q_{T1}}{\pi} \Phi_g(x_1, t_1, \mu^2) \int \frac{dx_2}{x_2} \int \frac{d^2q_{T2}}{\pi} \Phi_g(x_2, t_2, \mu^2) \times \\ \times d\hat{\sigma}^{PRA}(RR \rightarrow J/\psi\gamma) \quad (1)$$

where  $q_{1,2} = x_{1,2}P_{1,2} + q_{1,2T}$  are 4-momenta of Reggeized gluons,  $P_{1,2}^\mu = \frac{\sqrt{s}}{2}(1, 0, 0, \pm 1)$  are 4-momenta of protons,  $q_{1,2T} = (0, \mathbf{q}_{1,2T}, 0)$  are transverse 4-momenta of gluons,  $t_{1,2} = -\mathbf{q}_{1,2T}^2$ ,  $\Phi_g(x, t, \mu^2)$  is the uPDF of the Reggeized gluon. Note, the modified KMRW uPDF satisfied exact normalization condition at the arbitrary  $x$ ,<sup>18</sup>

$$\int_0^{\mu^2} \Phi_g(x, t, \mu^2) dt = x f_g(x, \mu^2). \quad (2)$$

The parton-parton cross-section  $d\hat{\sigma}^{PRA}(RR \rightarrow J/\psi\gamma)$ , as well as  $d\hat{\sigma}^{PRA}(RR \rightarrow \psi'\gamma)$  and  $d\hat{\sigma}^{PRA}(RR \rightarrow \chi_{cJ}\gamma)$ , are written via the squared Reggeized amplitude  $|\overline{M}|_{PRA}^2$  by a usual textbook formula, see (8) and (13).

The parton-parton scattering amplitudes in the PRA are calculated using the Feynman rules of the Lipatov EFT. Within this framework, the amplitudes are gauge-invariant and the initial-state partons are treated as Reggeized partons. To obtain Reggeized amplitudes, we use in our calculations the Mathematica package FeynArts<sup>38</sup> and the corresponding model file ReggeQCD by Maxim Nefedov.<sup>17</sup>

The gauge invariance of all amplitudes has been verified additionally. Furthermore, the squared amplitudes in the PRA have an explicit collinear limit, which has been verified analytically for each considered squared amplitudes as follows

$$\lim_{t_1, t_2 \rightarrow 0} \int_0^{2\pi} \int_0^{2\pi} \frac{d\phi_1 d\phi_2}{(2\pi)^2} \overline{|M|^2}_{PRA} = \overline{|M|^2}_{CPM}. \quad (3)$$

The PRA has been used to describe the production of direct and prompt  $J/\psi$  mesons in high energy proton-proton collisions. In previous studies, we have found good agreement between the LO PRA computation and experimental data from the CDF, ATLAS, CMS, and LHCb collaborations.<sup>19–21,39–41</sup>

### 3. PRA using NRQCD

The approach of NRQCD is a theoretical framework that separates the effects of short-distance and long-distance physics. The cross section of the charmonium  $\mathcal{C}$  production in the gluon-gluon fusion can be expressed as a sum over all possible states of a  $c\bar{c}$ -pair with respect to the quantum numbers, see Ref.:<sup>9</sup>

$$\sigma(RR \rightarrow \mathcal{C}\gamma) = \sum_n \hat{\sigma}(RR \rightarrow c\bar{c}[n]\gamma) \frac{\langle O^{\mathcal{C}}[n] \rangle}{N_{col} N_{pol}} \quad (4)$$

where  $[n] = [^{2S+1}L_J^{(1,8)}]$  is the state of a  $c\bar{c}$ -pair, written using the usual spectroscopic notation. The quantum number in upper index <sup>(1,8)</sup> identifies color singlet or color octet states, respectively. The  $\hat{\sigma}$  represents the partonic cross-section for the production of the state  $c\bar{c}[n]$ , and  $\langle O^{\mathcal{C}}[n] \rangle$  are the long-distance matrix element (LDME), which describes the transition of an intermediate state into a charmonium  $\mathcal{C}$ . One has  $N_{col} = 2N_c$  for the color-singlet states and  $N_{col} = N_c^2 - 1$  for the color-octet states,  $N_{pol} = 2J + 1$ .

To study prompt  $J/\psi$  production we take into consideration the direct production in the subprocess

$$R + R \rightarrow J/\psi + \gamma, \quad (5)$$

and the cascade production in the subprocesses

$$R + R \rightarrow \psi' + \gamma \quad (6)$$

$$R + R \rightarrow \chi_{cJ} + \gamma, \quad (7)$$

via  $\psi' \rightarrow J/\psi X$  and  $\chi_{cJ} \rightarrow J/\psi\gamma$  decays. At the LHC energies  $J/\psi + \gamma$  production subprocesses in the quark-antiquark annihilation give small contributions and may be neglected. We derive analytical formulae for the relevant Reggeized amplitudes using FeynArts and ReggeQCD packages. The corresponding squared amplitudes are unwieldy for the presentation here and they may be obtained from authors by the request.

The master formula for the numerical calculation in the PRA can be obtained from the factorization formula (1) and the partonic cross-section

$$d\hat{\sigma}^{PRA}(RR \rightarrow J/\psi\gamma) = (2\pi)^4 \delta^{(4)}(q_1 + q_2 - p_\psi - k_\gamma) \frac{|\overline{M}|_{PRA}^2}{I} \frac{d^3 p_\psi}{(2\pi)^3 2p_\psi^0} \frac{d^3 k_\gamma}{(2\pi)^3 2k_\gamma^0}, \quad (8)$$

where  $I = 2x_1 x_2 s$  is the flux factor,  $p_\psi^\mu$  is the  $J/\psi$  4-momentum,  $k_\gamma$  is the photon 4-momentum. In such a way, in the PRA using the NRQCD we can write for direct  $J/\psi + \gamma$  production cross-section

$$\frac{d\sigma(pp \rightarrow J/\psi\gamma X)}{dp_{\psi T} dy_\psi dk_{\gamma T} dy_\gamma d\Delta\phi} = \frac{p_{\psi T} k_{\gamma T}}{16\pi^3} \int dt_1 \int d\phi_1 \Phi_g(x_1, t_1, \mu^2) \Phi_g(x_2, t_2, \mu^2) \frac{|\overline{M}|_{PRA}^2}{(x_1 x_2 s)^2} \quad (9)$$

where  $\mathbf{q}_{2T} = \mathbf{p}_T + \mathbf{k}_T - \mathbf{q}_{1T}$ ,  $x_1 = (p_\psi^0 + k_\gamma^0 + p_\psi^z + k_\gamma^z)/\sqrt{s}$ ,  $x_2 = (p_\psi^0 + k_\gamma^0 - p_\psi^z - k_\gamma^z)/\sqrt{s}$ ,  $y_\psi$  is the  $J/\psi$  rapidity,  $y_\gamma$  is the photon rapidity,  $\Delta\phi = \phi_\psi - \phi_\gamma$ . Squared amplitudes  $|\overline{M}|_{PRA}^2$  are written as functions of conventional Mandelstam variables  $\hat{s}, \hat{t}, \hat{u}$  and variables  $t_1, t_2, a_k, a_p, b_k, b_p$ , where  $a_k = 2(k_\gamma \cdot P_2)/s$ ,  $a_p = 2(p_\psi \cdot P_2)/s$ ,  $b_k = 2(k_\gamma \cdot P_1)/s$ ,  $b_p = 2(p_\psi \cdot P_1)/s$ .

#### 4. PRA using ICEM

In the PRA using the ICEM, the description of the associated production of  $J/\psi$  and large- $p_T$  direct photon at the leading order in  $\alpha_S$  is possible via the subprocesses

$$R + R \rightarrow c + \bar{c} + \gamma \quad (10)$$

and

$$Q + \bar{Q} \rightarrow c + \bar{c} + \gamma. \quad (11)$$

However, the latter subprocess contributes negligibly (see Fig. 1), and therefore, it can be ignored.

In the ICEM, the prompt  $J/\psi$ -meson production cross-section may be written in the following manner:

$$\sigma(pp \rightarrow J/\psi\gamma X) = F^\psi \int_{m_\psi^2}^{4m_D^2} \frac{d\sigma(pp \rightarrow c\bar{c}\gamma X)}{dM^2} dM^2 \quad (12)$$

where  $M$  is the  $c\bar{c}$ -pair invariant mass,  $m_D$  is the mass of the lightest  $D$ -meson. In other words, the integration is carried out from the charmonium mass up to the open charm production threshold. The ICEM takes into account the fact that the mass of the intermediate state (i.e. the invariant mass of the  $c\bar{c}$ -pair) differs from the mass of the  $J/\psi$  meson and the relation between 4-momenta should be accounted  $p_\psi^\mu = p^\mu \frac{m_\psi}{M}$ , here  $p^\mu = p_c^\mu + p_{\bar{c}}^\mu$ . In the study of prompt  $J/\psi$  production at the LHC using the PRA plus ICEM approach, it was found that a good description of the data may be archived with hadronization parameter  $F^\psi \simeq 0.02$  at the  $\sqrt{s} = 13$  TeV.<sup>22</sup>

The cross-section for the subprocess (4) is written the same as (8) taken into account that it is 2 → 3 parton-level process:

$$d\hat{\sigma}^{PRA}(R + R \rightarrow c + \bar{c} + \gamma) = (2\pi)^4 \delta^{(4)}(q_1 + q_2 - p_c - p_{\bar{c}} - k_\gamma) \frac{|\overline{M}|_{PRA}^2}{2x_1 x_2 s} \times \\ \times \frac{d^3 p_c}{(2\pi)^3 2p_{c0}} \frac{d^3 p_{\bar{c}}}{(2\pi)^3 2p_{\bar{c}0}} \frac{d^3 k_\gamma}{(2\pi)^3 2k_{\gamma 0}}. \quad (13)$$

The master formula for numerical calculations in the PRA using the ICEM, obtained from (12) and (13), reads

$$\frac{d\sigma(pp \rightarrow J/\psi \gamma X)}{dp_{\psi T} dy_\psi dk_{\gamma T} dy_\gamma d\Delta\phi} = F^\psi \times \frac{p_{\psi T} k_{\gamma T}}{1024\pi^6} \int_{m_\psi}^{4m_D^2} dM^2 \int dt_1 \int d\phi_1 \int d\Omega_{c\bar{c}} \left(\frac{M}{m_\psi}\right)^2 \times \\ \times \sqrt{1 - \frac{4m_c^2}{M^2}} \Phi_g(x_1, t_1, \mu^2) \Phi_g(x_2, t_2, \mu^2) \frac{|\overline{M}|_{PRA}^2}{(x_1 x_2 s)^2}, \quad (14)$$

where  $d\Omega_{c\bar{c}} = \sin(\theta)d\theta d\phi$ , angles  $\theta$  and  $\phi$  are associated with the rest frame of the  $c\bar{c}$ -pair,<sup>18</sup> and we put during numerical calculations the mass of  $c$ -quark is equal  $m_c = 1.3$  GeV, the mass of  $D$ -meson -  $m_D = 1.86$  GeV, and the mass of  $J/\psi$  -  $m_\psi = 3.097$  GeV.

It is suitable for numerical calculation to rewrite  $c$ -quark (antiquark) 4-momenta as follows,

$$p_c^\mu = \frac{1}{2}p^\mu + r^\mu \text{ and } p_{\bar{c}}^\mu = \frac{1}{2}p^\mu - r^\mu, \quad (15)$$

where 4-momentum of relative motion  $r^\mu$  is written in terms of invariant mass  $M$ ,  $c\bar{c}$ -pair transverse momentum  $p_T$  and  $c\bar{c}$ -pair rapidity  $y$ . Such a way,

$$r^\mu = \frac{1}{2} \sqrt{M^2 - 4m_c^2} (X^\mu \sin(\theta) \cos(\phi) + Y^\mu \sin(\theta) \sin(\phi) + Z^\mu \cos(\theta)), \quad (16)$$

where

$$X^\mu = \frac{1}{M} \left( p_T \cosh(y), \sqrt{M^2 + p_T^2}, 0, p_T \sinh(y) \right), \\ Y^\mu = \text{sign}(y) (0, 0, 1, 0), \\ Z^\mu = \text{sign}(y) (\sinh(y), 0, 0, \cosh(y)).$$

The squared amplitude  $|\overline{M}|_{PRA}^2$  is calculated using FeynArts and ReggeQCD packages and may be written as a function of  $\hat{s} = (q_1 + q_2)^2$ ,  $\hat{t} = (q_1 - k)^2$ ,  $\hat{u} = (q_2 - k)^2$ ,  $w_1 = (q_1 - p_c)^2$ ,  $w_2 = (q_2 - p_{\bar{c}})^2$ ,  $a_c = 2(p_c \cdot P_2)/s$ ,  $a_{\bar{c}} = 2(p_{\bar{c}} \cdot P_2)$ ,  $a_k = 2(k_\gamma \cdot P_2)$ ,  $b_c = 2(p_c \cdot P_1)/s$ ,  $b_{\bar{c}} = 2(p_{\bar{c}} \cdot P_1)$ ,  $b_k = 2(k_\gamma \cdot P_1)$ .

The calculation in the PRA using the ICEM, as they are explained above, may be performed in a different way within the Monte-Carlo event generator KaTie,<sup>42</sup> the same as in Ref.<sup>43</sup> for the process of the associated  $J/\psi$  plus  $Z(W)$ -boson production. We have done cross-check all calculations in the PRA using the ICEM within the KaTie, and found a good agreement.

## 5. Results

Now, we are in a position to discuss the results of the numerical calculations in which we compare predictions obtained in the PRA using the NRQCD and in the PRA using the ICEM.

In the first step, we calculate  $J/\psi + \gamma$  production cross section in the PRA using the NRQCD when  $J/\psi$  is produced directly via different intermediate color-singlet and color-octet states. The results are shown in Fig. 1(a). We confirm the well-known conclusion on the dominant role of color-singlet production mechanism in the direct  $J/\psi + \gamma$  production.<sup>1,3</sup> In Fig. 1 (a), we plot total contribution from the quark-antiquark annihilation subprocesses included both color-singlet and color-octet production mechanisms additionally and find that it is very small at the  $\sqrt{s} = 13 - 14$  TeV. Taking in mind experimental difficulties in the separation of the direct and the prompt  $J/\psi$  production processes, we estimate  $J/\psi + \gamma$  production cross-section when  $J/\psi$  is produced in cascade processes via decays of the excited charmonium state,  $\psi(2S) \rightarrow J/\psi X$  and  $\chi_{cJ} \rightarrow J/\psi\gamma$ . We see in Fig. 1 (b) that only  $J/\psi$  production via  $\psi(2S)$  decay may be important with the contribution in a few percent in the prompt  $J/\psi + \gamma$  production cross-section. Such a way, we will take into account the NRQCD approach only color-singlet contribution, i.e. we will use the CSM.<sup>7,8</sup> The contributions from cascade productions will be also neglected such as small ones in comparing with the theoretical uncertainties of the PRA calculations.

To validate our results additionally, we compare them with the NLO CPM using the CSM calculations at the energy  $\sqrt{s} = 14$  TeV published in Ref.<sup>6</sup> We calculate the transverse momentum spectrum of the  $J/\psi$ -mesons for the kinematic conditions  $|y_\psi|, |y_\gamma| < 3$  and  $p_{T\gamma} > 5$  GeV, which were used in Ref.<sup>6</sup> We find the PRA using the CSM calculation sufficiently overestimates the NLO CPM using the CSM cross-section at all  $J/\psi$  transverse momenta, see Fig. 1 (c). This is an interesting finding because in the single  $J/\psi$  production the results obtained in the LO PRA and the NLO CPM using the NRQCD are approximately coincided. The significant disparity has also been identified in the PRA predictions made using different hadronization models, the  $p_T$ -spectrum obtained in the ICEM is sufficiently lower than the spectrum obtained in the CSM starting from small  $p_{\psi T}$  up to  $p_{\psi T} = 30$  GeV. The NLO CPM using the ICEM calculations are absent and we can't compare NLO CPM predictions obtained using different hadronization models.

The total cross-sections as functions of the  $p_{T\gamma}^{min}$  are shown in Fig. 1(d). The prediction of the PRA using the CSM is larger the prediction of the NLO CPM using the CSM at small  $p_{T\gamma}^{min}$  because we integrate over the  $p_{T\psi} > 10$  GeV where the NLO CPM using the CSM prediction strongly suppressed when  $p_{T\gamma}$  is small due to the mostly back-to-back production of the  $J/\psi$  and photon is dominant in the CPM instead of the PRA. In Fig. 1 and below, the theoretical uncertainties due to variations in the hard scale by a factor of 2 is indicated by shaded regions.

Taking into account the relatively small contribution of color-octet states and cascade production of  $J/\psi$ -meson, the predictions were made in the PRA using the

CSM for the LHC energy  $\sqrt{s} = 13$  TeV in the central rapidity region  $|y_{J/\psi}|$  and  $|y_\gamma| < 2$ . In Fig. 2, the differential cross sections are shown as functions of the  $J/\psi$  transverse momentum  $p_{\psi T}$ , photon transverse momentum  $p_{\gamma T}$ ,  $J/\psi$  rapidity  $y_\psi$ , photon rapidity  $y_\gamma$ , rapidity difference  $\Delta y = |y_\psi - y_\gamma|$  and azimuthal angle difference  $\Delta\phi = |\phi_\psi - \phi_\gamma|$ . Solid curves are the PRA using CSM calculations, dashed curves are the PRA using ICEM calculations. In Fig. 3, the differential cross-sections are shown as functions of the invariant mass  $M = M_{\psi\gamma}$ , transverse momentum difference  $\mathcal{A}_T = (|\mathbf{p}_{\psi T}| + |\mathbf{p}_{\gamma T}|) / (|\mathbf{p}_{\psi T}| + |\mathbf{p}_{\gamma T}|)$ , pair transverse momentum  $p_T = |\mathbf{p}_{\psi T} + \mathbf{p}_{\gamma T}|$  and pair rapidity  $Y = Y_{\psi\gamma}$ .

## 6. Conclusions

Working in the PRA, we confirm previously obtained results that in the process of the associated  $J/\psi$  and direct photon production the CSM approximation of the NRQCD is the dominant contribution and we can neglect color-octet contributions. The second general finding is that we can neglect small contributions from the quark-antiquark annihilation processes to calculate  $J/\psi$  plus photon production cross-section at the energy  $\sqrt{s} = 13 - 14$  TeV. We find surprising sufficient differences in predictions based on the CSM and the ICEM which become larger when the photon transverse momentum increases. The ICEM prediction is strongly suppressed relative the CSM prediction instead of good agreement between the ICEM and the NRQCD calculations for the single  $J/\psi$  prompt production. In such a way, experimental measurement of the  $J/\psi$  plus large- $p_T$  photon production cross-section could be potentially used to distinguish between the ICEM and the NRQCD.

## 7. Acknowledgments

The work is supported by the Foundation for the Advancement of Theoretical Physics and Mathematics BASIS, grant No. 24-1-1-16-5 and by the grant of the Ministry of Science and Higher Education of the Russian Federation, No. FSSS-2024-0027.



## References

1. M. Drees and C. S. Kim, *Z. Phys. C* **53**, 673 (1992).
2. T. Mehen, *Phys. Rev. D* **55**, 4338 (1997).
3. M. A. Doncheski and C. S. Kim, *Phys. Rev. D* **49**, 4463 (1994).
4. W. J. den Dunnen, J. P. Lansberg, C. Pisano and M. Schlegel, *Phys. Rev. Lett.* **112**, 212001 (2014).
5. M. Butenschoen and B. A. Kniehl, *Mod. Phys. Lett. A* **28**, 1350027 (2013).
6. R. Li and J.-X. Wang, *Phys. Lett. B* **672**, 51 (2009).
7. R. Baier and R. Ruckl, *Z. Phys. C* **19**, 251 (1983).
8. E. L. Berger and D. L. Jones, *Phys. Rev. D* **23**, 1521 (1981).
9. G. T. Bodwin, E. Braaten and G. P. Lepage, *Phys. Rev. D* **51**, 1125 (1995), [Erratum: *Phys.Rev.D* **55**, 5853 (1997)].
10. H. Fritzsch, *Phys. Lett. B* **67**, 217 (1977).
11. F. Halzen, *Phys. Lett. B* **69**, 105 (1977).
12. Y.-Q. Ma and R. Vogt, *Phys. Rev. D* **94**, 114029 (2016).
13. J. Collins, *Foundations of Perturbative QCD*, Cambridge Monographs on Particle Physics, Nuclear Physics and Cosmology, Vol. 32 (Cambridge University Press, 7 2023).
14. J. C. Collins, D. E. Soper and G. F. Sterman, *Factorization of Hard Processes in QCD* 1989 pp. 1–91.
15. M. G. Echevarria, T. Kasemets, J.-P. Lansberg, C. Pisano and A. Signori, *Phys. Lett. B* **781**, 161 (2018).
16. M. A. Nefedov, V. A. Saleev and A. V. Shipilova, *Phys. Rev. D* **87**, 094030 (2013).
17. A. V. Karpishkov, M. A. Nefedov and V. A. Saleev, *Phys. Rev. D* **96**, 096019 (2017).
18. M. A. Nefedov and V. A. Saleev, *Phys. Rev. D* **102**, 114018 (2020).
19. B. A. Kniehl, D. V. Vasin and V. A. Saleev, *Phys. Rev. D* **73**, 074022 (2006).
20. V. A. Saleev, M. A. Nefedov and A. V. Shipilova, *Phys. Rev. D* **85**, 074013 (2012).
21. B. A. Kniehl, M. A. Nefedov and V. A. Saleev, *Phys. Rev. D* **94**, 054007 (2016).
22. A. A. Chernyshev and V. A. Saleev, *Phys. Rev. D* **106**, 114006 (2022).
23. N. Brambilla *et al.*, *Eur. Phys. J. C* **71**, 1534 (2011).
24. W. Vogelsang and M. R. Whalley, *J. Phys. G* **23**, A1 (1997).
25. ATLAS Collaboration, G. Aad *et al.*, *JHEP* **11**, 169 (2021).
26. ALICE Collaboration, S. Acharya *et al.*, *Eur. Phys. J. C* **79**, 896 (2019).
27. CMS Collaboration, A. M. Sirunyan *et al.*, *Eur. Phys. J. C* **79**, 20 (2019).
28. V. A. Saleev, *Phys. Rev. D* **78**, 114031 (2008).
29. B. A. Kniehl, V. A. Saleev, A. V. Shipilova and E. V. Yatsenko, *Phys. Rev. D* **84**, 074017 (2011).
30. M. Nefedov and V. Saleev, *Phys. Rev. D* **92**, 094033 (2015).
31. A. Karpishkov and V. Saleev, *Phys. Rev. D* **106**, 054036 (2022).
32. J. C. Collins and R. K. Ellis, *Nucl. Phys. B* **360**, 3 (1991).
33. S. Catani and F. Hautmann, *Nucl. Phys. B* **427**, 475 (1994).
34. L. V. Gribov, E. M. Levin and M. G. Ryskin, *Phys. Rept.* **100**, 1 (1983).
35. L. N. Lipatov, *Nucl. Phys. B* **452**, 369 (1995).
36. M. A. Kimber, A. D. Martin and M. G. Ryskin, *Phys. Rev. D* **63**, 114027 (2001).
37. G. Watt, A. D. Martin and M. G. Ryskin, *Eur. Phys. J. C* **31**, 73 (2003).
38. T. Hahn, *Comput. Phys. Commun.* **140**, 418 (2001).
39. V. A. Saleev, M. A. Nefedov and A. V. Shipilova, *Phys. Rev. D* **85**, 074013 (2012).
40. M. A. Nefedov, V. A. Saleev and A. V. Shipilova, *Phys. Atom. Nucl.* **76**, 1546 (2013).
41. V. A. Saleev, M. A. Nefedov and A. V. Shipilova, *Phys. Rev. D* **85**, 074013 (2012).
42. A. van Hameren, *Comput. Phys. Commun.* **224**, 371 (2018).

43. A. Chernyshev and V. Saleev, *Int. J. Mod. Phys. A* **38**, 2350193 (2023),  
[arXiv:2304.07481 \[hep-ph\]](#).

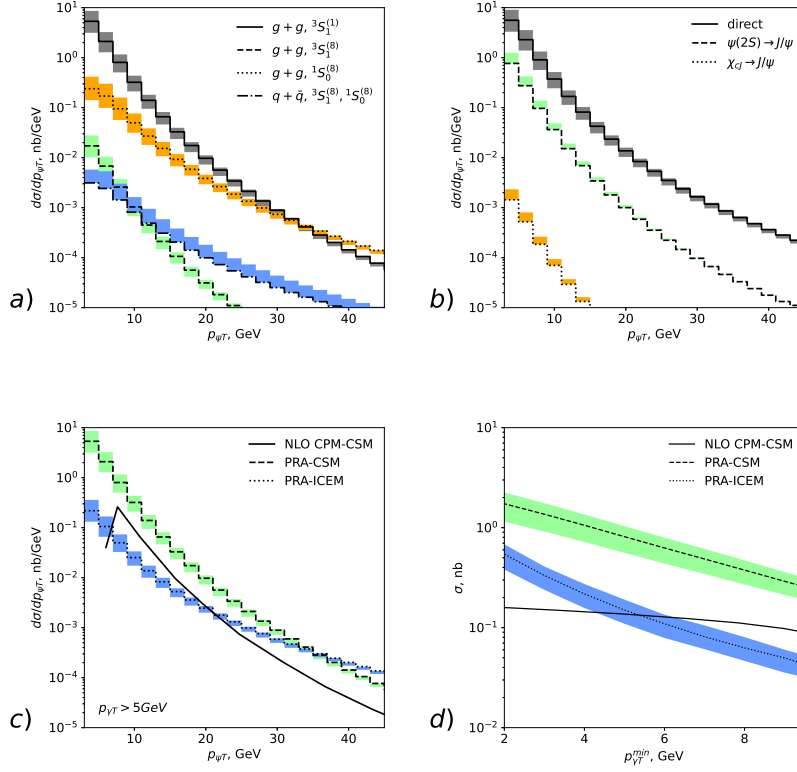


Fig. 1. Cross-section for the associated production of  $J/\psi + \gamma$  as a function of the  $p_{\psi T}$  at the  $\sqrt{s} = 14$  TeV obtained in the PRA using the NRQCD at  $|y_{\gamma, \psi}| < 2$ . In the panel (a), solid curve — the CSM contribution, dashed curve — the contribution of the color octet  $[^1S_0^{(8)}]$  state, dotted curve — the contribution of color-octet  $[^3S_1^{(8)}]$  state and the contribution of quark-antiquark annihilation processes are shown as a dashed blue curve. In the panel (b), solid curve — the direct  $J/\psi$  production, dashed curve — the cascade via  $\psi(2S) \rightarrow J/\psi X$  production, dotted curve — the cascade via  $\chi_{cJ} \rightarrow J/\psi \gamma$  production. In the panel (c), solid curve — the NLO CPM using the CSM calculation from Ref.,<sup>6</sup> dashed curve — the PRA using the CSM calculation and dotted curve — the PRA using the ICEM calculation. In the panel (d), cross-section for the associated production of  $J/\psi + \gamma$  as a function of the  $p_{\gamma T min}$  at the  $p_{\psi T} > 10$  GeV. Solid curve — the NLO CPM using the CSM calculation from Ref.,<sup>6</sup> dashed curve — the PRA using the CSM calculation and dotted curve — the PRA using the ICEM calculation.

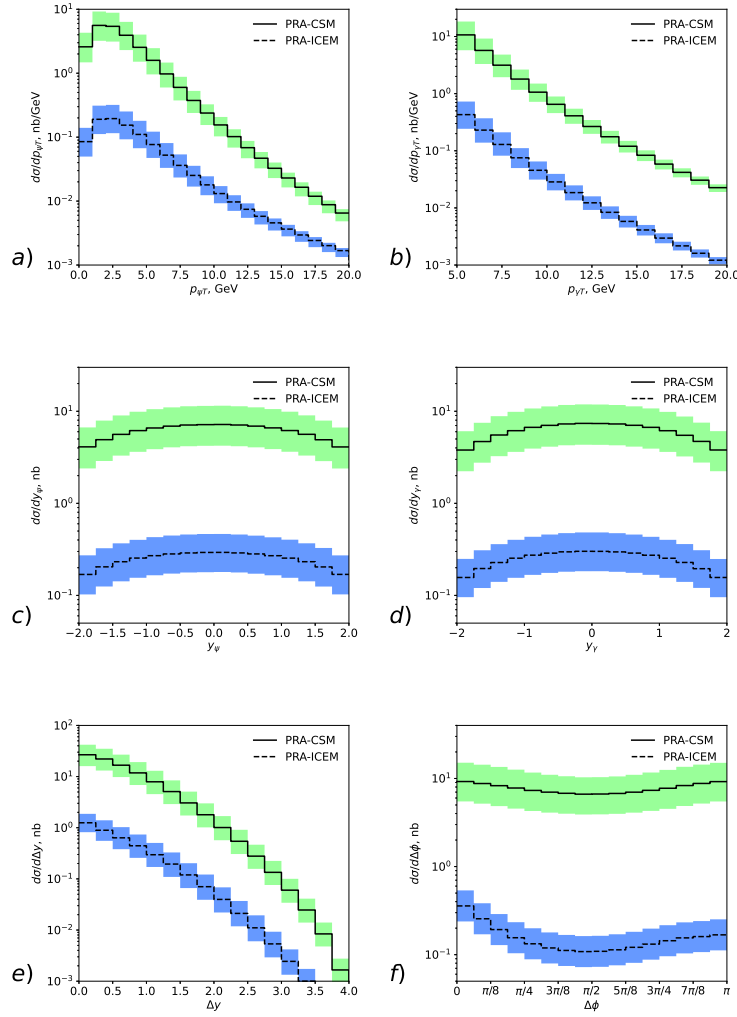


Fig. 2. Differential cross-sections for the associated production of  $J/\psi + \gamma$  at the  $\sqrt{s} = 13$  TeV and  $|y_{\gamma, \psi}| < 2$  as functions of the  $p_{\psi T}$  (a),  $p_{\gamma T}$  (b),  $y_{\psi}$  (c),  $y_{\gamma}$  (d), rapidity difference  $\Delta y$  (e) and azimuthal angle difference  $\Delta\phi$  (f). Solid curves are the PRA using CSM calculations, dashed curves are the PRA using ICEM calculations.

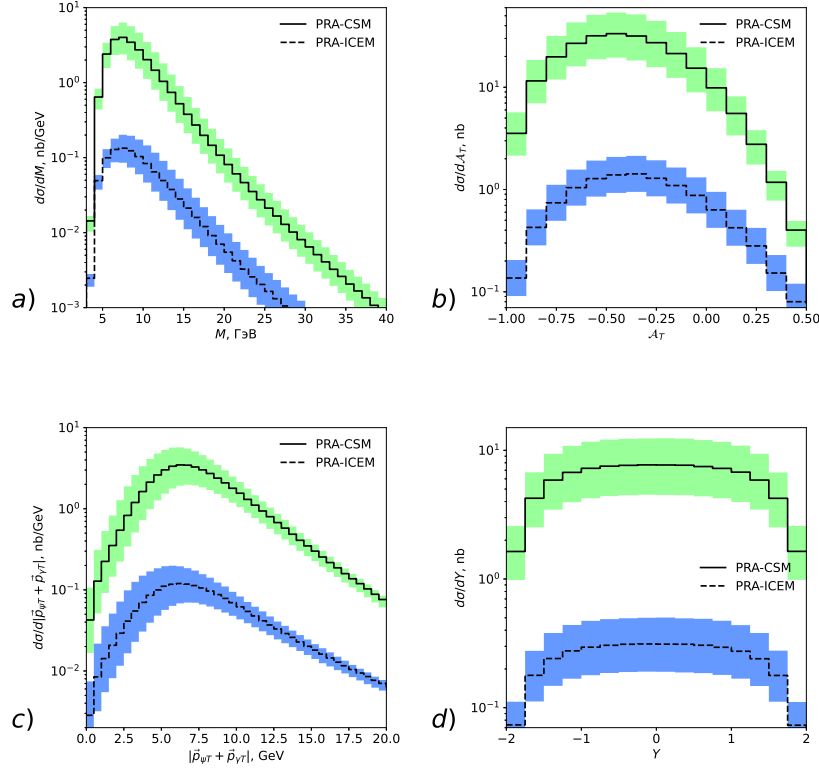


Fig. 3. Differential cross-sections for the associated production of  $J/\psi + \gamma$  at the  $\sqrt{s} = 13$  TeV and  $|y_{\gamma, \psi}| < 2$  as functions of the invariant mass  $M = M_{\psi\gamma}$  (a), transverse momentum difference  $\mathcal{A}_T$  (b), pair transverse momentum  $p_T = |\mathbf{p}_{\psi T} + \mathbf{p}_{\gamma T}|$  (c) and pair rapidity  $Y_{\gamma\psi}$  (d). Solid curves are the PRA using CSM calculations, dashed curves are the PRA using ICEM calculations.